FULL TITLE
*ASP Conference Series, Vol. **VOLUME**, **YEAR OF PUBLICATION***
NAMES OF EDITORS

Dust in the HD 38529 Planetary System

Amaya Moro-Martín,[1] Renu Malhotra,[2] John M. Carpenter,[3]
Lynne A. Hillenbrand,[3] Sebastian Wolf,[4] Michael R. Meyer,[5]
David Hollenbach,[6] Joan Najita,[7] and Thomas Henning [4]

[1]*Dep. of Astrophysical Sciences, Princeton University, Princeton, NJ 08544*
[2]*Dep. of Planetary Sciences, University of Arizona, 1629 E. University Boulevard, Tucson, AZ 85721*
[3]*Dep. of Astronomy, California Institute of Technology, Pasadena, CA 91125*
[4]*Max-Planck-Institut für Astronomie, Königstuhl 17, 69117 Heidelberg, Germany*
[5]*Steward Observatory, University of Arizona, 933 N. Cherry Ave., Tucson, AZ 85721*
[6]*NASA Ames, Moffet Field, CA 94035*
[7]*National Optical Astronomy Observatory, 950 N. Cherry Ave., Tucson AZ 85721*

Abstract. In this paper we briefly sumarized a study on HD 38529, one of the few (less than a dozen) stars known to date to harbor both planetary companions and IR excess, the later due to debris dust and evidence of the presence of planetesimals. For details, please refer to Moro-Martín et al. 2007b.

1. Introduction

HD 38529 is a 3.5 Gyr old (Valenti & Fischer 2005 and Gonzalez et al. 2001) post-main sequence G8III/IV star that harbors two planets having $M\sin i$ of 0.8 M_{Jup} and 12.2 M_{Jup}, semimajor axes of 0.13 AU and 3.74 AU, and eccentricities of 0.25 and 0.35, respectively (Butler et al. 2006). This system is of particular interest because *Spitzer* observations have shown an excess emission above the stellar photosphere, with a signal-to-noise ratio (S/N) at 70 μm of 4.7, a small excess at 33 μm (S/N=2.6) and no excess <30 μm (Moro-Martín et al. 2007a). In this paper we constrain the distribution of the potential dust-producing planetesimals from the study of the dynamical perturbations of the two known planets, considering in particular the effect of secular resonances. This allows us to identify three regions where planetesimals could be dynamically stable (§2). We show how we can further constrain the location of the dust (and the parent planetesimals) by modeling HD 38529 spectral energy distribution (SED – §3). In §4 we discuss together the results from the dynamical and SED analysis and summarize our findings.

2. Possible Location of the Dust-Producing Planetesimals: Effect of Gravitational Perturbations by the Planets

We can identify the possible location of the dust-producing planetesimals by studying the effect of the planetary perturbations on the stability of the planetesimals' orbits. First, we can eliminate planetesimals with orbits that would cross the orbits of the planets. Second, we note that planetesimals in initially circular orbits would be strongly unstable in the vicinity of the orbits of each of the two known planets, in a range of semimajor axis, $\Delta a \simeq \pm 1.5(m_{\rm planet}/m_{\star})^{2/7}$ (Duncan et al. 1989). These two considerations identify several regions where planetesimals could not be stable, shown as the grey and red shaded zones in Fig. 1 (left panel). In addition, we need to consider the effect of secular perturbations, operating over much longer timescales, which can cause a strong eccentricity excitation of the planetesimals, particularly at secular resonance locations, that can significantly shorten their lifetime. We study the effect of the secular resonances following the Laplace-Lagrange secular perturbation analysis (Murray and Dermott 1999; Malhotra (1998 - see details in Moro-Martín et al. 2007b). The results are shown in Fig. 1 (left panel) for test particles in initially circular orbits. Clearly, very significant secular eccentricity excitation occurs over a wide zone that extends to distances much larger than the unstable zones identified above. Remarkably, even though the strongly unstable zone of the outer planet extends outward to only about 5.5 AU, the eccentricity excitation exceeds 0.3 to more than 10 AU. In general, we see that the forced eccentricities exceed 0.1 everywhere up to $\sim$ 57 AU. A strong secular resonance with the slow mode occurs at a semimajor axis value of $\sim$ 55 AU, where the particles become planet-crossing or can even collide with the star. Thus, tentatively, we can identify three regions that could harbor planetesimal populations (or perhaps small planets) in low eccentricity orbits, and could therefore be potential sources of dust: an inner region 0.4–0.8 AU in-between the two planets' orbits, and two outer regions, 20–50 AU and beyond 60 AU. This conclusion is confirmed by numerical integrations of test particles using a symplectic integrator (see Moro-Martín et al. 2007b). To find out which of these dynamically stable niches do actually show signs of harboring dust-producing plantesimals we turn now to the study of the IR excess emission detected by *Spitzer*.

3. SED Modeling

For the modeling of the observed SED, we use the radiative transfer code developed by Wolf & Hillenbrand (2003). We model the dust disk as an annulus of inner radius R_{in}, outer radius R_{out}, total dust mass M_{dust}, and a constant surface density ($\Sigma \propto r^0$, so that the number density, $n(r) \propto r^{-1}$). We assume that the dust grains are composed of silicates with optical constants from Weingartner & Draine (2001). For the particle sizes we consider two options: 1) a single grain size of 10 μm in radius, and 2) a particle size distribution following a power law, $n(b) \propto b^{-q}$, where b is the particle radius, $q = 3.5$ (for grains in collisional equilibrium), $b_{min} = 2$ μm (the minimum size of the grains that can remain bound in the system) and $b_{max} = 10$ μm. In both cases, the radius of 10 μm was chosen because such a grain radiates efficiently at 70 μm. Because

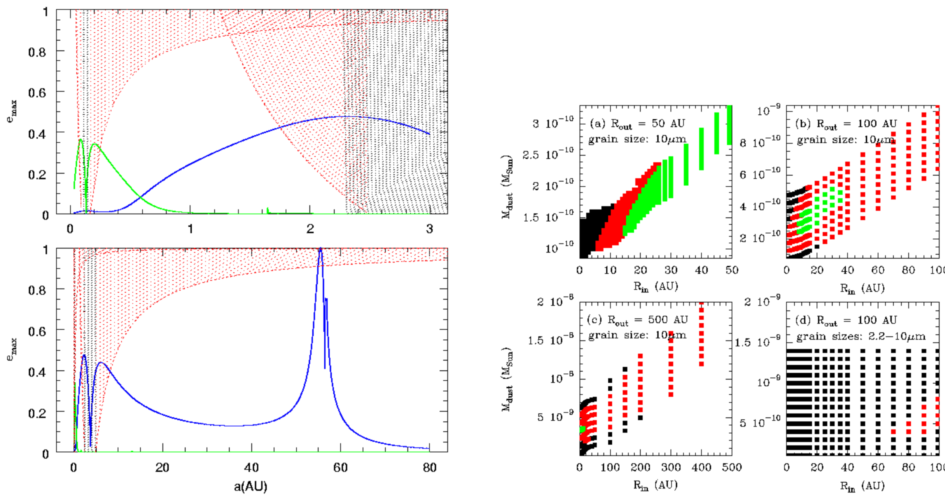

Figure 1. *Left*: Test particle orbits are unstable in the red and grey-shaded zones, due to planet crossing orbits and overlapping first order mean motion resonances, respectively. The secular modes of the two planets, HD38529b and HD38529c, excite the eccentricities of circular test particle orbits: the maximum eccentricity due to the fast mode is shown by the green curve, while that due to the slow mode is shown by the blue curve. *Right*: Each point represents a modeled SED, where R_{in} and M_{dust} are the two free parameters. (a)–(c) Models with a single grain size of 10 μm and with R_{out} = 50 AU, 100 AU and 500 AU, respectively. (d) Models with a distribution of grain sizes given by $n(b) \propto b^{-3.5}$, with $b_{min} = 2$ μm and $b_{max} = 10$ μm. The *green*, *red* and *black* points show models with $P(\chi^2 \mid \nu) < 0.683$, > 0.683 and > 0.9973, respectively. Models in black can be excluded with 3-σ certainty. The red dots in (d) have $P(\chi^2 \mid \nu) > 0.988$ and therefore they are all close to be excluded with a 3-σ certainty, i.e. we can exclude the presence of a significant population of small grains inside 100 AU based on the lack of a significant continuum emission at $\lambda < 30$ μm.

of the last property, this choice of grain size provides a lower limit for M_{dust}. The outer radius of the disk, R_{out}, cannot be constrained with data currently available. Based on scattered-light observations from nearby debris disks, we consider disk sizes of R_{out} = 50 AU (Solar System size), R_{out} = 100 AU and R_{out} = 500 AU. With the above three values for R_{out}, assuming a uniform density distribution and with the grain size and composition fixed, we then vary R_{in} and M_{dust} (our only two free parameters) to create a grid of models where we allow R_{in} to vary from the silicate sublimation radius (R_{sub}, where T_{sub} = 1550 K) to R_{out} (Fig. 1 – right panel). This accounts for the possibility of having either a dust disk of wide radial extent or a narrow ring of dust. Some of these SEDs are shown in Fig. 2 together with the observations.

To evaluate whether a particular model is a valid fit to the Spitzer observations, or if not, to what degree of certainty the model can be excluded, we calculate its χ^2 probability, $P(\chi^2 \mid \nu)$, where ν is the number of degrees of freedom. In our case $\nu = 2$, as the only two free parameters are R_{in} and M_{dust}, and all the other disk parameters and dust properties are fixed to the values given above. The probability is defined so that $P(0 \mid \nu) = 0$ and $P(1 \mid \nu) = 1$. Models with $P(\chi^2 \mid \nu) > 0.9973$ can be excluded with a 3-σ certainty, while models with $P(\chi^2 \mid \nu) > 0.683$ could be excluded with a 1-σ certainty (see Fig. 1 – right panel).

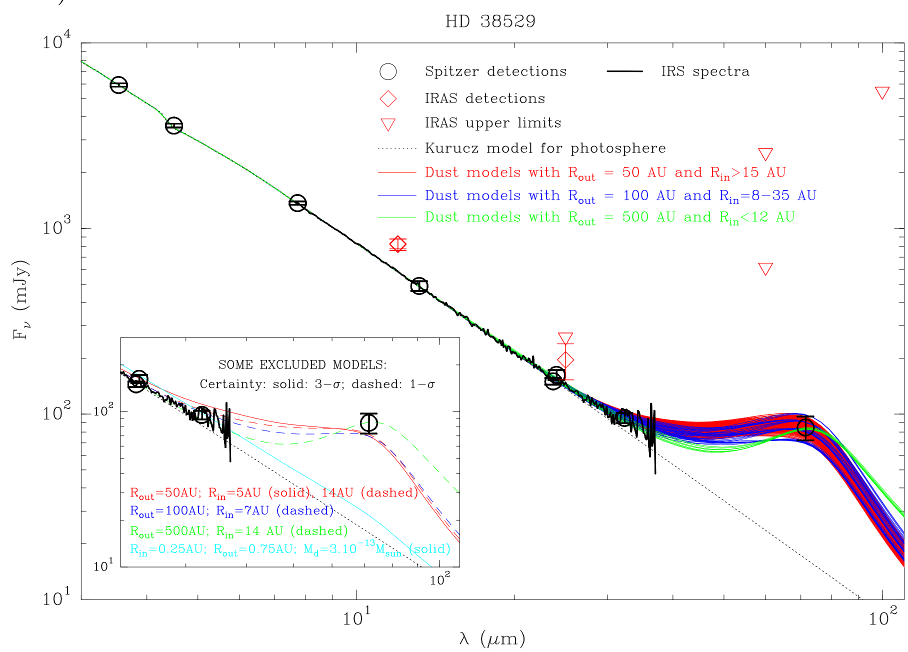

Figure 2. Observed (black thick line and symbols) and modeled (colored lines) SEDs for HD 38529. The colored continuous lines in the main panel show three sets of models that fit the observations with a χ^2 probability < 0.68 (corresponding to the models represented in *green* in Fig. 1 – right panel). The models include the emission from the photosphere and from a dust disk composed of astronomical silicate grains 10 μm in radius. We assume the dust disk extends from R_{in} to R_{out} with a constant surface density. We consider three values for R_{out}: 50 AU (*red*), 100 AU (*blue*) and 500 AU (*green*). R_{in} and M_{dust} are allowed to vary. The insert at the lower left shows the most relevant excluded models. The solid line represents models excluded with a certainty of 3-σ, while the dashed line corresponds to 1-σ. The model shown in *light blue* gives an upper limit to the amount of warm dust located between 0.25–0.75 AU.

4. Discussion

The two outermost regions identified in §2 where planetesimals could survive for extended periods of time in the presence of the two known radial velocity-detected planets, namely 20–50 AU and beyond 60 AU, are in broad agreement with the allowed dust locations that result from the modeling of the SED described in §3. In particular, the models with R_{out} = 50 AU predict an inner cavity of radius > 5 AU; while a range of dust disks with R_{out} = 50 AU and R_{in} > 20 AU could fit the observed SED. From the models with R_{out} = 100 AU, we can conclude that it is very unlikely that the observed dust emission arises only from planetesimals located beyond 60 AU because the models with R_{out} = 100 AU and R_{in} = 60 AU, 70 AU, 80 AU and 90 AU have $P(\chi^2 \mid \nu)$ larger than 0.83, 0.87, 0.89 and 0.91, respectively A similar conclusion can be drawn from the models with R_{out} = 500 AU, and $R_{in} > 60$ AU, for which $P(\chi^2 \mid \nu) >$ 0.94. Therefore, from the dynamical and SED modeling we conclude that the planetesimals responsible for most of the dust emission are likely located within the 20–50 AU region (with a dust mass estimate of 1–5$\times10^{-10}$ $M_\odot$ of 10 μm particles). In this regard, HD 38529 resembles the configuration of the Solar System's Jovian planets + Kuiper Belt (KB).

The lack of an IR excess at wavelengths shorter than 30 μm allows us to place an upper limit on the amount of warm (asteroidal) dust that could be located in the modestly stable small zone in-between the two known planets (0.4–0.8 AU). We find that a 3-σ upper limit to the dust mass in this potential asteroid belt is 3×10^{-13} $M_\odot$ or 10^{-7} $M_\oplus$. For comparison, the mass estimate for the zodiacal cloud in the terrestrial planet region of the Solar System is 3×10^{-10} $M_\oplus$ (Hahn et al. 2002), i.e. 330 times smaller than the estimated upper limit of warm dust in HD 38529.

Acknowledgments

We thank the rest of the FEPS team members, colleagues at the Spitzer Science Center, and members of all the Spitzer instrument teams for advice and support. This work is based on observations made with the Spitzer Space Telescope, which is operated by the Jet Propulsion Laboratory, California Institute of Technology unders NASA contrast 1407. A.M.M. is under contract with the Jet Propulsion Laboratory (JPL) funded by NASA through the Michelson Fellowship Program. JPL is managed for NASA by the California Institute of Technology. A.M.M. is also supported by the Lyman Spitzer Fellowship at Princeton University.

References

Butler, R.P., Wright, J.T., Marcy, G.W. et al. 2006, ApJ, 646, 505
Duncan, M., Quinn, T. & Tremaine, S. 1989, Iracus, 82, 402
Gonzalez, G., Laws, C., Tyagi, S. et al. 2001, ApJ, 121, 432
Hahn, J.M., Zook, H.A., Cooper, B. & Sunkara, B. 2002, Icarus, 158, 360
Malhotra, R. 1998,in ASP Conf. Ser. 149, Solar System Formation and Evolution, ed. D. Lazzaro, R. Vieira Martins, S. Ferraz-Mello, J. Fernandez and Beauge, (San Francisco: ASP), 37
Moro-Martín, A., Carpenter, J.M., Meyer, M.R., Hillenbrand, L.A., Malhotra, R. et al. 2007, ApJ, 658, 1312
Moro-Martín, A., Malhotra, R., Carpenter, J.M., Hillenbrand, Wolf, S. et al. 2007, ApJ, 668, in press.
Murray, N. & Dermott, S., 1999, *Solar System Dynamics*, Cambridge University Press.
Valenti, J.A. & Fischer, D.A. 2005, ApJS, 159, 141
Weingartner, J.C. & Draine, B.T., 2001, ApJ, 548, 296
Wolf, S. & Hillenbrand, L.A. 2003, ApJ, 596, 603